Fluid-Dynamic and Mass-Transfer Behavior of Static Mixers and Regular Packings

Omar N. Cavatorta and Ursula Böhm
Dept. de Industrias, Universidad de Buenos Aires, Ciudad Universitaria, 1428 Buenos Aires, Argentina

Ana María Chiappori de del Giorgio
Escuela de Ingeniería Química, Universidad Central de Venezuela, Apartado 54506, Caracas 1052A, Venezuela

The fluid dynamics and liquid-to-wall mass transfer for spaced and stacked regular packings were studied for forced convection and fluidized beds. The behavior of these configurations in bubble columns and under natural convection conditions is also presented. Flow parameters characterizing structured packings, presented in the literature, were used in the evaluation of results. General equations to predict pressure drop and mass transfer are discussed, as well as the relationship between energy dissipation and mass transfer. In the presence of fluidized particles, single-phase flow or natural convection conditions, the mass-transfer behavior of a packing element stacked between other packs or separated from the neighboring elements by liquid layers is almost the same, but differs in bubble columns.

Introduction

In recent years regular (or structured) packings have been incorporated in a large variety of industrial equipment as a way of improving fluid-dynamic behavior, enhancing efficiency, assessing concentration and temperature homogeneity, lowering energy costs, and so on.

In thermal separation processes, for instance, the use of structured packings proved to increase the capacity, to enhance separation performance, and to save energy as compared to conventional packings. The packing elements, consisting of thin corrugated sheets, are inserted in the column, filling the whole cross section. The different packing elements are stacked close together and each packing layer is turned 90° in relation to the previous one in order to achieve a good radial mixing. In the present article this way of assembling will be called ‘‘regular packing’’ (RP). In other processes, as for instance reactive distillation, oxidizing of organic products or bioreactions in bubble columns, where a high dispersion degree is essential, the same packing elements are placed in the equipment with liquid layers between the different packs. In this work the term ‘‘static mixer’’ (SM) denotes the arrays of separated regular packing elements.

Correspondence concerning this article should be addressed to U. Böhm.

Moreover, regular packings are used as catalyst support in chemical reactors (Agar and Ruppel, 1988) or as support of microorganisms in biofilm reactors (Spekuljak et al., 1994). When large equipment is required, application of this type of reactor will be more suitable than the use of conventional fluidized-bed reactors. The latter often present problems of hydrodynamic instabilities, especially when they operate at low liquid flow rates (that is, when small or light particles are fluidized, when the particle concentration is high, or when there is a need for long residence time of the liquid phase).

For the design of chemical or biological reactors that use regular packings as support of catalysts, enzymes, or bacteria, the knowledge of fluid to packing mass-transfer coefficients is essential. Since these reactors may operate in the presence of suspended particles or dispersed bubbles and at low liquid throughputs, it is of interest to determine mass-transfer coefficients for these conditions and to compare the values obtained with both regular packings and static mixers. Results obtained in previous research dealing with single-phase flow (Colazo et al., 1991), fluidized particles (Colazo and Böhm, 1992), bubble beds (Tasat et al., 1995; Neme et al., 1997), and natural convection (Rey et al., 1998), all with regular packings, are also considered for comparison.

Table 1. Experimental Conditions

Characteristics of Packing Sheets Packing Material: Pure Nickel*							
Packing**	α [°]	β [°]	a [cm^{-1}]	a' [cm]	b [cm]	Dh [cm]	Z [cm]
A	95.0	30	8.20	0.572	0.85	0.314	5.00
B	106.5	40	8.24	0.562	0.90	0.286	4.00
C	82.4	45	5.68	0.532	0.70	0.297	4.42
D	106.5	50	8.37	0.542	0.90	0.286	4.00
E	97.0	60	8.05	0.567	0.85	0.308	4.00
F	75.0	42	7.34	0.602	0.73	0.360	4.92

Geometric Configurations								
Code	RP30	RP′42	RP45	SM25	SM34	SM50	SM′50	SM′100
Packing	A	F	C	A	A	A	F	F
X [cm]	0	0	0	2.5	3.4	5.0	5.0	10.0

Flow Configurations	Packings
Forced convection	A, C, F
Fluidized bed	A, C
Natural convection	A, B, C, D, E
Bubble column	C, F
	A, B, D, E (plastic)

Characteristics of Particles Material: Glass Shape: Spherical		
dp [cm]	0.0534	0.100
ρp [$g \cdot cm^{-3}$]	2.612	2.737

*Packings A, B, D and E were also made from plastic.
**Packings A–E: smooth plates, average $\epsilon = 0.88$; packing F: perforated plates (70 orifices of 0.046 cm diameter per cm^2) $\epsilon = 0.95$.

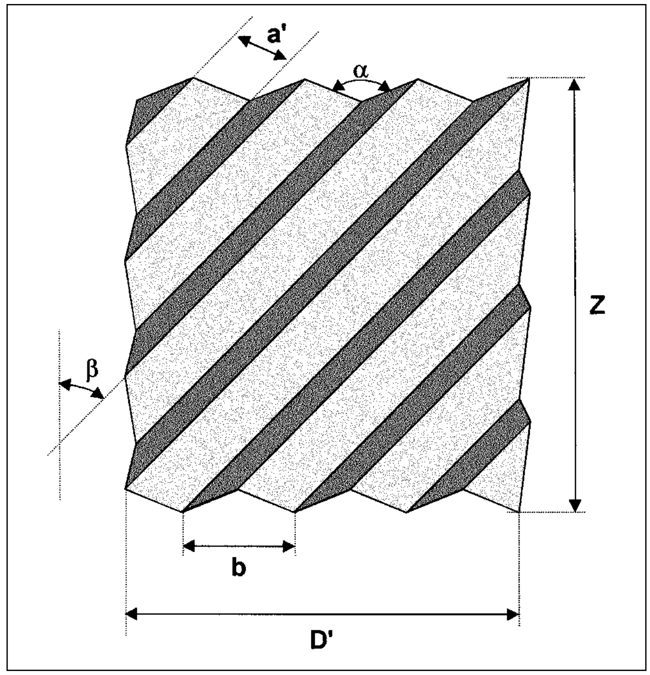

Figure 1. Geometric parameters of corrugated sheets.

Experimental Apparatus and Procedure

All the experimental results presented in this investigation were obtained with regular packings and static mixers of the Sulzer SMV type. Table 1 gives their characteristics and Figure 1, showing one corrugated sheet, defines the different geometric parameters. Table 1 also includes the characteristics of particles used in the fluidization experiments.

Mass-transfer coefficients were determined by the electrochemical technique (Selman and Tobias, 1978). Limiting current intensities were measured on two or three electrically active corrugated plates inside the packing element. The remaining plates of the pack were insulated by epoxy coating or were replaced by similar corrugated plastic plates. The adjacent pack, with all the sheets in electrical contact, worked as the cell counterelectrode. The packings were made of pure nickel, according to the requirements of the electrochemical method employed. The test reaction was the reduction of ferricyanide ions in an alkaline medium. All the solutions contained the redox pair potassium ferri/ferro-cyanide; the supporting electrolyte was either sodium hydroxide or a buffer of sodium carbonate-bicarbonate. To some of the solutions carboxymethyl cellulose sodium salt was added in order to modify their viscosity. The composition and physical properties at 25°C of the different electrolytic solutions are detailed in Table 2.

The experiments were performed using a circular column (with 0.05 m ID and that is 0.75 m high) or a square section column (0.04 m × 0.04 m × 0.35 m) both made of Lucite. Inside the column the packing elements were stacked close together (RP) or with liquid layers of varying depth between them (SM). The different arrangements studied and the corresponding codes are given in Table 1.

The experimental series correspond to the following flow conditions: forced convection, fluidized bed, natural convection, and bubble column. The equipment is shown in Figure 2.

In the forced-flow tests, performed with and without fluidized particles, the electrolyte was circulated through the column from a constant-temperature reservoir by means of a

Table 2. Composition and Physical Properties at 25°C of Employed Solutions

Code		S1	S2	S3	S4	S5	S6
$\{Fe(CN)_6\}^{-3}$	[$kmol \cdot m^{-3}$]	0.001	0.01	0.01	0.001	0.001	0.001
$\{Fe(CN)_6\}^{-4}$	[$kmol \cdot m^{-3}$]	0.001	0.02	0.02	0.001	0.001	0.001
NaOH	[$kmol \cdot m^{-3}$]	0.5	2.0	3.0	—	—	—
Na_2CO_3	[$kmol \cdot m^{-3}$]	—	—	—	0.4	0.4	0.4
$NaHCO_3$	[$kmol \cdot m^{-3}$]	—	—	—	0.4	0.4	0.4
CMC*	[$kg \cdot m^{-3}$]	—	—	—	1.0	1.5	3.0
Density	[$kg \cdot m^{-3}$]	1023	1083	1121	1068	1069	1069
Viscosity	[$mPa \cdot s$]	1.004	1.30	1.75	1.85	2.19	3.50
Diffusivity	[10^{-10} $m^2 \cdot s^{-1}$]	7.42	5.90	4.34	5.30	5.28	5.25

*Carboxymethylcellulose sodium salt.

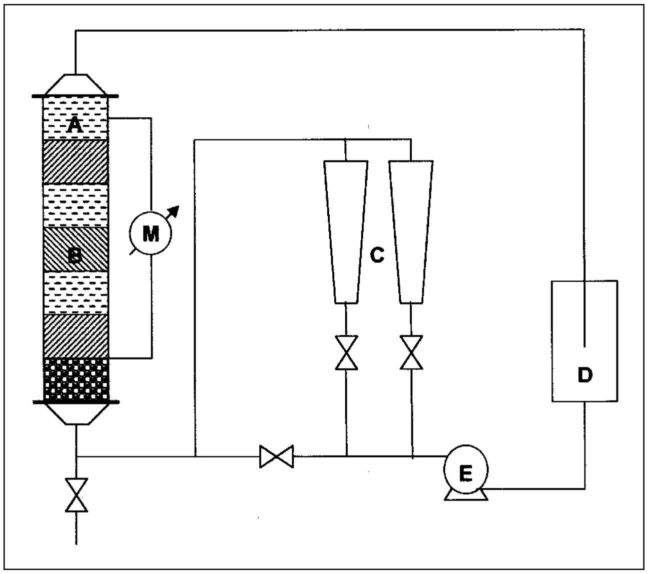

Figure 2. Experimental equipment.

(A) column; (B) packing; (C) flowmeters; (D) tank; (E) pump; (M) manometer.

centrifugal pump. The flow rate was measured by flowmeters. For the natural convection measurements, the column without connecting pipelines was placed in a thermostat for better control of the electrolyte temperature.

In the bubble column, the liquid operated in the batch mode. The gas phase was humidified nitrogen, introduced in the column through an orifice sparger with a single hole of 1 mm diameter.

Experimental details and particular operating conditions, if not described here, may be found elsewhere in the publications previously mentioned.

Forced Convection in Single Phase

This situation was investigated with packing elements built of smooth metal sheets having corrugation inclination angles of 30° and 45°; both types were installed as regular packings. The former packing elements were used for the static mixer tests. Practically all solutions described in Table 2 were employed.

Fluid-dynamic behavior

Theoretical (Spekuljak and Billet, 1989) and semiempirical (Bravo et al., 1986) approaches to the problem of estimating the pressure drop through regular packings can be found in the literature. Friction factors based on these models were evaluated from the experimental data of pressure drop obtained by manometric measurement. The pressure taps were placed one at the base of the column and the other 0.30 m downstream, as shown in Figure 2.

Since pressure drop is mainly due to friction on the corrugated metal sheets, the pressure drop per unit length of packing present in the column, as well as an interstitial liquid flow velocity and a hydraulic diameter of the flow channels, are used in the calculations. Figures 3a and 3b illustrate the modes of friction-factor prediction corresponding to the

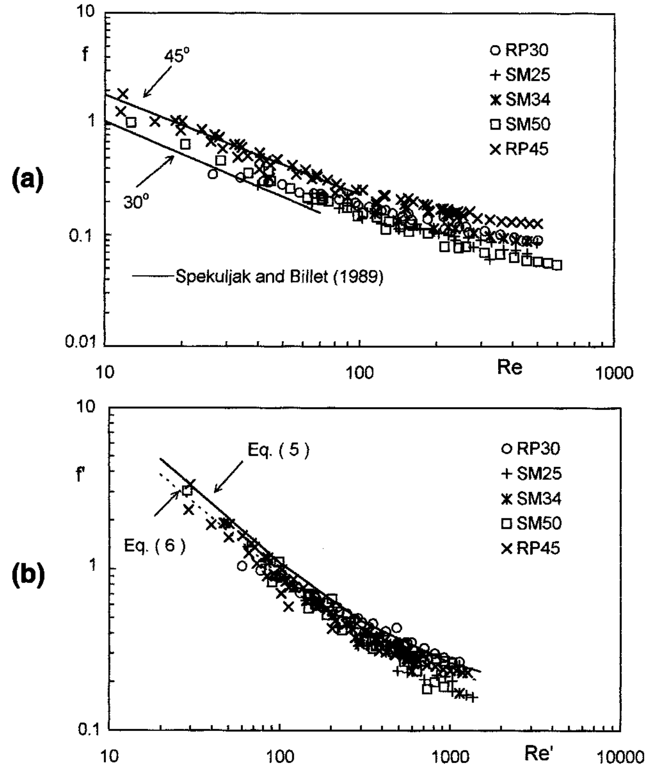

Figure 3. Friction factor for regular packings and static mixers.

(a) f and Re as defined by Spekuljak and Billet (1989); (b) f' and Re' as defined by Bravo et al. (1986).

models presented by Spekuljak and Billet (1989) and by Bravo et al. (1986), respectively. In the former case the friction factor is evaluated from pressure drop data by the following equation:

$$f = \frac{1}{2}\frac{\Delta P}{L}\frac{D_h}{\rho v^2}, \tag{1}$$

where

$$v = \frac{Vs}{\epsilon} \tag{2}$$

is the interstitial velocity, and the hydraulic diameter is

$$D_h = \frac{d' \sin\alpha}{1+\sin\left(\dfrac{\alpha}{2}\right)}. \tag{3}$$

Meanwhile, in the second case,

$$f' = \frac{\Delta P}{L}\frac{D'_h}{\rho v'^2}, \tag{1'}$$

with

$$v' = \frac{Vs}{\epsilon\cos\beta} \tag{2'}$$

and

$$D_h' = d'. \tag{3'}$$

The experiments covered the laminar and transition flow regime. According to an expression derived by Zogg (1972):

$$Re_{\mathrm{tr}} = \frac{511.67 - 7\beta}{\epsilon\left[1 + \sin\left(\dfrac{\alpha}{2}\right)\right]}, \tag{4}$$

the limit between these two regimes would occur at $Re = 197$ with the packing having a corrugation inclination angle of $\beta = 30°$, and at $Re = 135$ for $\beta = 45°$ (Figure 3a).

No marked differences in results were observed with the packs stacked together and the static mixers. This means that friction generated inside the packing element is predominant over pressure losses due to inlet/outlet flow at each pack of the static mixer.

The theoretical model of Spekuljak and Billet (1989) yields a different relationship for each corrugation inclination angle. Furthermore it includes particular coefficients (only listed for some commercial packings) and "nonmodeled" factors to describe the transition flow regime. However, in the laminar flow range a good agreement between predicted and experimental data of this work is found.

The method of Bravo et al. (1986), which takes into account the slope of the corrugations by defining an "effective" velocity inside the furrows, brings both sets of data together (Figure 3b). Although the present data fall below the general equation of Bravo,

$$f' = 0.171 + \frac{92.7}{Re'} \tag{5}$$

validated by pressure drop data for gauze packing, this advantageous form of correlation was adopted, leading to the following relationship:

$$f' = 0.148 + \frac{78.4}{Re'} \tag{6}$$

($N = 164$; $\delta = 9.8\%$), which may be used in the estimation of pressure drop through corrugated-sheet-metal packings and static mixers geometrically similar to those used in the present investigation.

Mass transfer

The same regular packings and static mixers used in the pressure-drop study were employed in the determination of mass-transfer coefficients in single-phase flow. The values obtained with the different active corrugated plates were averaged in order to describe the mass-transfer behavior of the whole pack. Figure 4a is obtained by expressing these results in the classic way of j-factor vs. Reynolds number.

As there is no definite influence of the distance between packs on mass transfer, all the data (RP and SM) with a corrugation inclination angle of 30° were correlated together, yielding the relationships given in Figure 4a. They hold for the laminar and the transition flow regime, respectively. Also shown are the data and analog equations derived in the previous work on mass transfer to regular packing with a corrugation inclination angle of 45° (Colazo et al., 1991). As can be observed, the values of j-factor differ systematically by about 25% for the two packings investigated, making it necessary to establish separate correlations for each corrugation inclination angle.

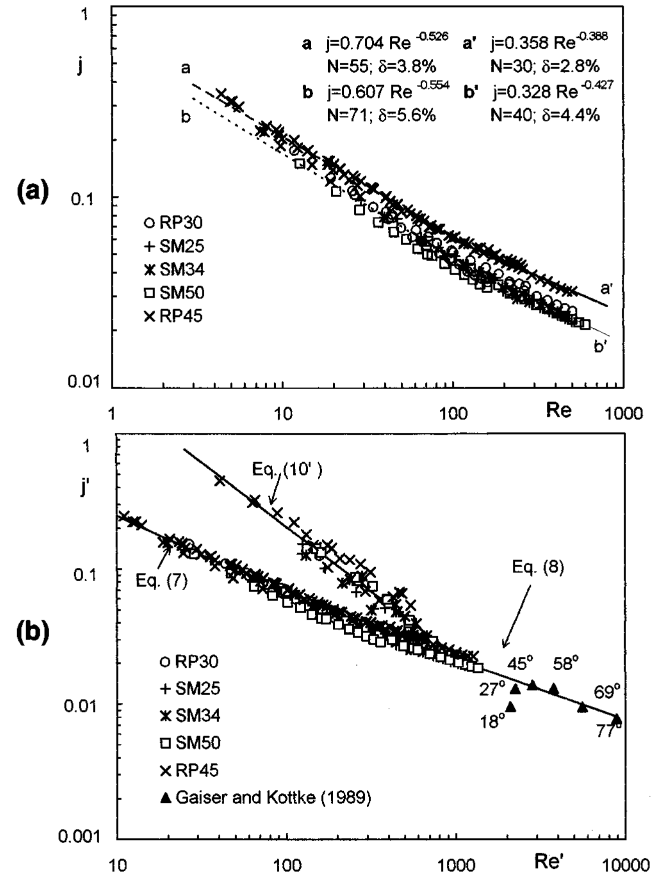

Figure 4. General mass-transfer correlation for regular packings and static mixers.

(a) Single-phase flow; flow parameters according to Spekuljak and Billet (1989); (b) single-phase flow and fluidized bed; flow parameters according to Bravo et al. (1986).

However, when the flow parameters proposed by Bravo et al. (1986), defined by Eqs. 2′ and 3′, are introduced, thus replacing

$$j = \frac{k}{v} Sc^{2/3}$$

by

$$j' = \frac{k \cos\beta}{v} Sc^{2/3}$$

and Re by Re', Figure 4b is obtained.

The data are well described by unique correlations for each flow regime:

$$j' = 0.927\ Re'^{-0.572} \qquad \text{for} \qquad Re' < 219 \tag{7}$$

($N = 89$; $R^2 = 0.974$; $\delta = 6.0\%$), and

$$j' = 0.443\ Re'^{-0.435} \qquad \text{for} \qquad 219 < Re' < 1360 \tag{8}$$

($N = 107$; $R^2 = 0.865$; $\delta = 7.8\%$).

Comparing the mean deviations (6% and 7.8%, respectively) with the somewhat lower deviations of the individual correlations, given in Figure 4a, it can be concluded that in view of the practical utility the accuracy of the general correlations (Eqs. 7 and 8) is acceptable.

The fact that the correlation coefficient for the curve fit diminishes from $R^2 = 0.974$ in the low Reynolds number range to $R^2 = 0.865$ in the transition regime may be explained as follows. It is well known that the inclination angle between the corrugated channels and the main flow direction is an essential parameter influencing heat or mass transfer, mixing quality, and residence-time characteristics inside the packing (Gaiser and Kottke, 1989; Focke et al., 1985; Spekuljak and Andrada, 1993; Heggs et al., 1997). This is taken into account partially through the effective velocity "$v \cos \beta$" in the furrows suggested by Bravo et al. (1986). But there also exist secondary swirling flows within the furrows due to the interaction of the crisscrossing streams, which are not considered in formulating the effective velocity. These swirl motions depend on the geometry of the structured packing and the flow velocity and become the main determinant in the heat or mass-transfer process as the flow velocity increases (Focke et al., 1985; Heggs et al., 1997). The lower correlation coefficient found with Eq. 8, valid in the transition and turbulent regime, may perhaps be attributed to this phenomenon. It should be pointed out that the established criterion between the different domains ($Re = 219$) was developed from equating the correlations in Eqs. 7 and 8, the transition from laminar to turbulent flow being gradual.

Gaiser and Kottke (1989), who examined flow phenomena and mass transfer for gases in corrugated passages of different structures, presented averaged mass-transfer coefficients for six corrugation inclination angles at a constant Reynolds number. These data, suitably transformed, are also shown in Figure 4b. It can be seen that, except for the value obtained at $\beta = 18°$, the results of Gaiser and Kottke (1989) can be well described by Eq. 8, indicating that the empirical correlation seems to be valid over a wider domain than specified and for corrugation inclination angles other than 30° and 45°.

Fluidized Beds

When particles are added to the systems studied with single-phase flow, the influence of the corrugation inclination angle practically disappears, as is illustrated below.

Fluid dynamic behavior

Figure 5a shows typical expansion curves obtained with glass spheres of 0.534 mm diameter fluidized in an empty

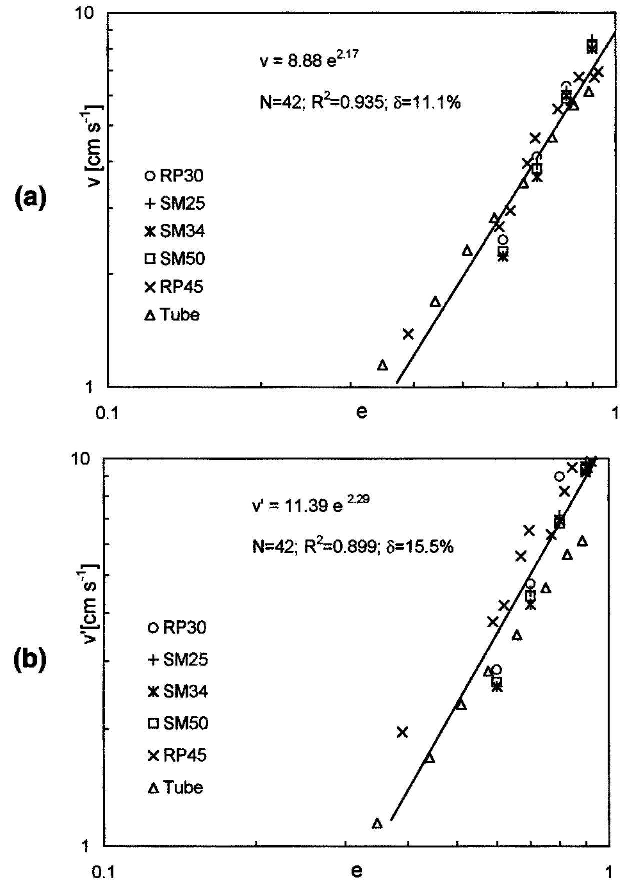

Figure 5. Expansion characteristics for fluidization in a tube and a column containing regular packing or static mixers.

(a) Flow parameters according to Spekuljak and Billet (1989); (b) flow parameters according to Bravo et al. (1986).

tube of 5 cm ID, and in columns containing regular packings with $\beta = 30°$ and $\beta = 45°$ and static mixers having the former corrugation slope and different liquid gaps between them. The interstitial flow velocity v is chosen in order to take into account the real flow section. As can be seen, the system geometry has no effect on the behavior of the fluidized bed. The corresponding expansion correlation is also given in Figure 5a. In this case, the representation of the expansion results in terms of the effective velocity v' will not improve the correlation, since the swirling action imposed on the crossing flows is enhanced by the moving particles. Indeed, as can be observed in Figure 5b the curve fit of the data points is even worse.

Mass transfer

It is well known that the presence of fluidized particles improves mass transfer to walls or to submerged objects. In the presence of structured packings the stirring generated by the particles, added to the mixing generated by the crossing flows, should enhance mass-transfer coefficients even more. But it was found that the effect of the fluidized particles is determinant; mass-transfer performance at the corrugated plates of regular packings or static mixers, with $\beta = 30°$ or $\beta = 45°$, is similar to that already described in the literature for other systems without packing elements. As previously observed, mass-transfer coefficients found in this research vary little with the fluidized-bed voidage, but present a slight maximum for a particle concentration of about 25%; they are strongly dependent on fluid viscosity and increase slightly when the particle diameter is increased. The most important finding, however, is that mass-transfer coefficients do not vary appreciably with the packing geometry. Therefore, relationships given in the literature for tube walls (King and Smith, 1967), annulus (Jagannadharaju and Rao, 1965; Tonini et al., 1981), maximum mass transfer to immersed objects (Böhm, 1983), describe the present results as well. Figure 6, for example, shows the results in the classic mode of correlation je vs. $Re_{dp}/(1-e)$.

The general equation

$$je = 0.333\left(\frac{Re_{dp}}{1-e}\right)^{-0.364} \tag{9}$$

($N = 68$; $\delta = 10.1\%$) compares satisfactorily to the relationships of King and Smith (1967):

$$je = 0.312\left(\frac{Re_{dp}}{1-e}\right)^{-0.375}, \tag{9'}$$

or of Jagannadharaju and Rao (1965):

$$je = 0.43\left(\frac{Re_{dp}}{1-e}\right)^{-0.380}. \tag{9''}$$

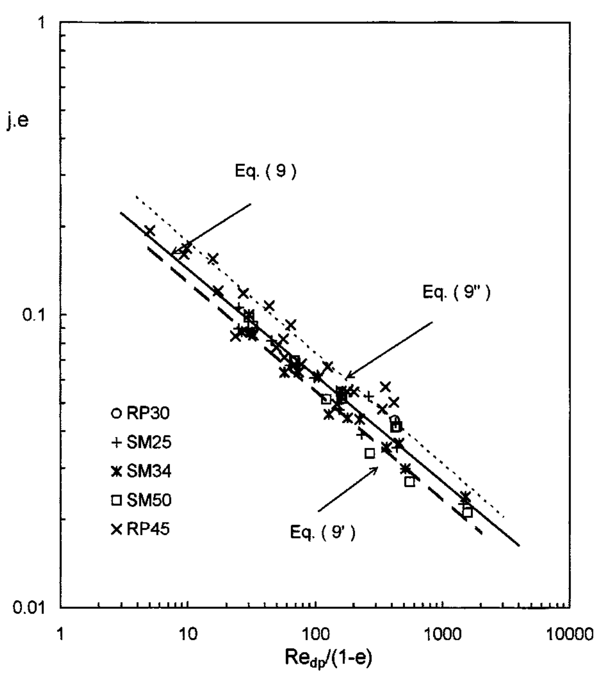

Figure 6. Mass transfer for regular packings and static mixers with fluidized particles; classic correlations.

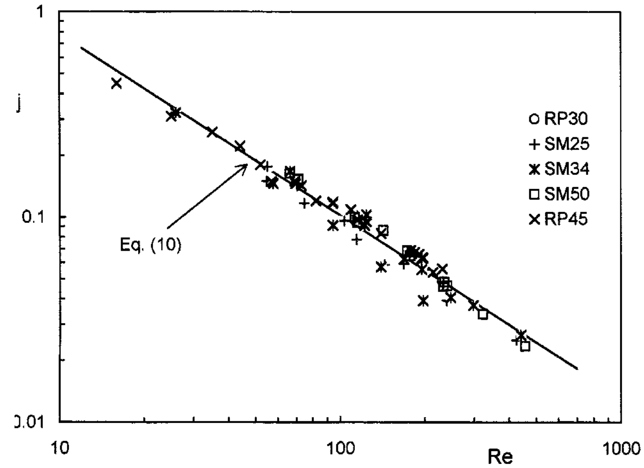

Figure 7. General mass-transfer correlation for regular packings and static mixers with fluidized particles.

In order to evaluate the enhancement of mass transfer in the presence of fluidized particles with respect to single-phase flow, results were also correlated in the same way as was described earlier for the experiments without solids. Figure 7 shows the experimental results in the form j-factor vs. Reynolds number. The corresponding empirical correlation is:

$$j = 6.02\,Re^{-0.885} \tag{10}$$

($N = 68$; $\delta = 9.2\%$).

When the same results are correlated as j'-factor with Re', the following relationship is derived:

$$j' = 16.40\,Re'^{-0.950} \tag{10'}$$

($N = 68$; $\delta = 11.4\%$).

This equation is plotted on Figure 4b for comparison purposes. The enhancement of the mass-transfer rate due to the presence of the fluidized solids is very important in the laminar flow regime (more than 200%) and decreases for the higher Reynolds numbers, that is, for low particle concentration.

Natural Convection

Although natural convection mass transfer in regular packings or in static mixers is not of practical interest, it appears in combination with forced convection at low flow rates. For instance, this situation will be found in bioreactors with microorganisms immobilized on the packing surface, which often operate at very low liquid velocities in order to obtain large residence times.

The correlations describing mass transfer by combined natural and forced convection are commonly based on a modified Reynolds number that includes a characteristic buoyancy-induced velocity added to the free stream velocity. The correlations may also apply the well-known coupling rule,

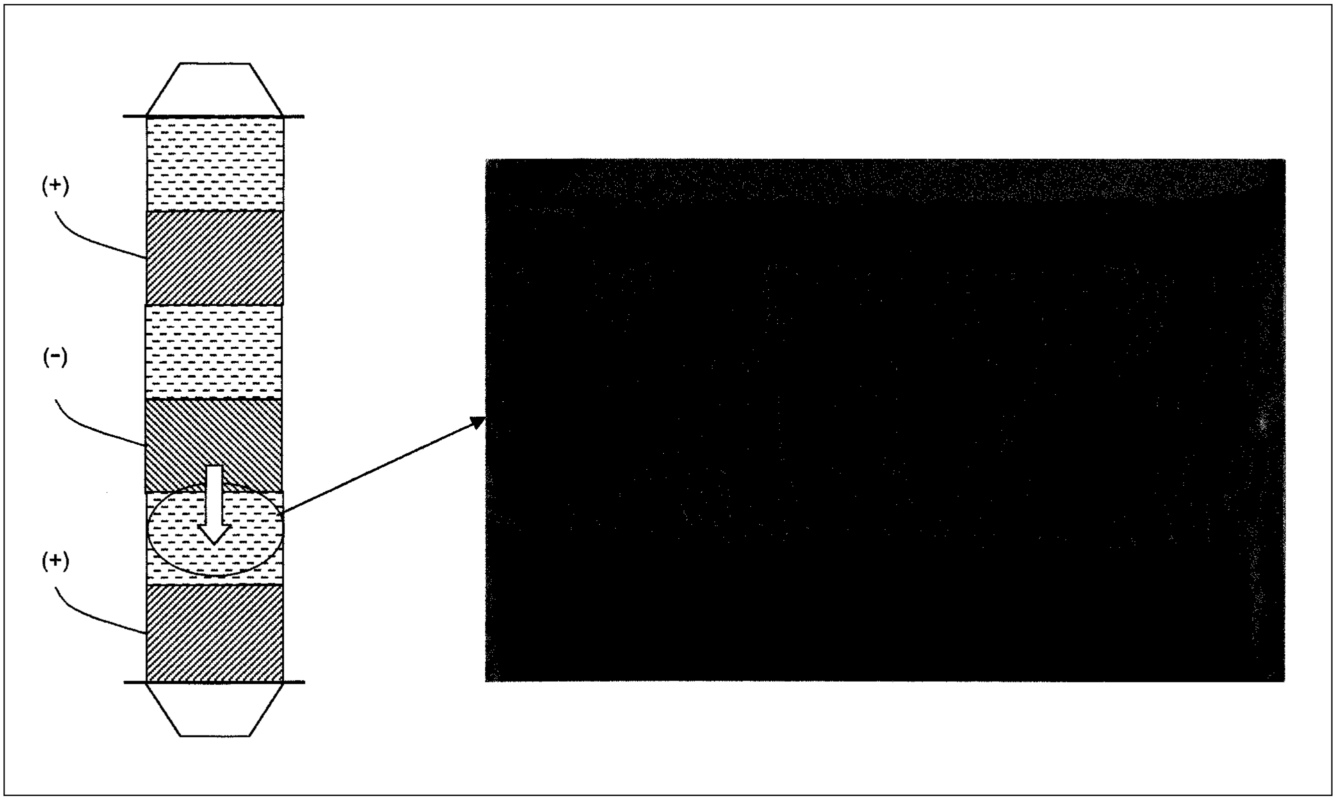

Figure 8. Flow pattern of natural convection streams leaving a static mixer (β = 60°, exposure time 15 s).

based on the power sum of individual Sherwood numbers corresponding to pure free and forced convection. This subject, applied to structured packings, was studied in detail and general correlations were derived elsewhere (Rey et al., 1998)

Fluid-dynamic behavior

Only in the case of a packing element working as a static mixer could some information on the convective flow structure be obtained. An optical method (Ibl and Müller, 1958) was applied in which a suspension of lycopodium particles is made visible by a laser beam spread into a vertical plane beneath the working static mixer, and the flow pattern is photographed. Since the mass-transfer reaction within the mixer involves a density increase at the transferring surface, the generated flow is downward and leaves the packing element at its bottom.

Figure 8 illustrates the complexity of the phenomenon. Although the impression is only two-dimensional, various types of flow are seen to occur: turbulence, swirling motion, and eddies, but also laminar streams leaving the static mixer at the channel intersections. Fluid velocities, calculated from the length of the luminous lines and the exposure time of the photographic frame, are up to five times greater than what would be obtained at a vertical plate under similar conditions.

Mass transfer

The natural convection study mentioned earlier (Rey et al., 1998), carried out with eight structured packings differing principally in packing height and channel inclination angle, yielded the following correlation:

$$Sh = 0.252\ (ScGr)^{0.299} \tag{11}$$

($N = 51;\ \delta = 2.3\%$).

Experiments with the packing elements separated from each other by 2.5 cm, 3.5 cm, or 5.0 cm (SM25, SM35, or

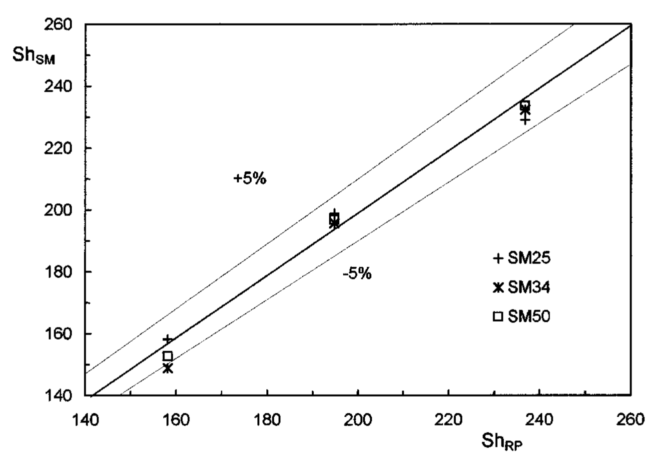

Figure 9. Natural convection mass transfer; comparison of experimental Sherwood numbers for static mixers with Sherwood numbers for regular packings.

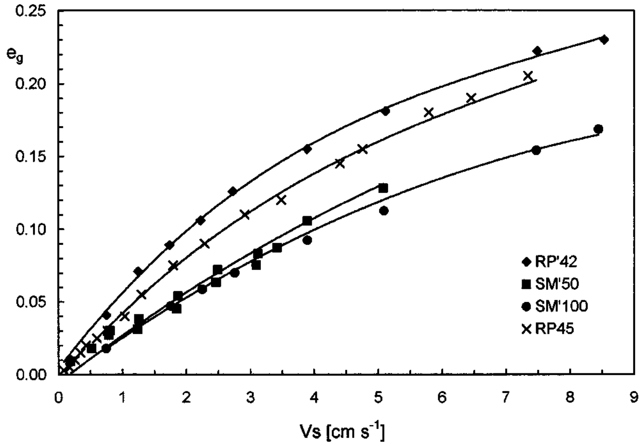

Figure 10. Gas holdup in bubble columns containing regular packing or static mixers (gas phase: nitrogen; liquid phase: distilled water).

SM50), yielded almost the same mass-transfer rates as those corresponding to the packs stacked together (RP30). Figure 9 shows that differences between Sherwood numbers obtained with the static mixers and with the regular packing are within 5%, so that Eq. 11 may be used indistinctly for both configurations, regular packings, or static mixers.

Bubble Columns

Experimental studies on the behavior of structured packings contained in bubble columns have been undertaken with the aim of deriving general mass-transfer correlations (Tasat et al., 1995; Neme et al., 1997). Regular packings made from smooth metal sheet (RP45) and from perforated plates (RP′42) were used and the influence of the gas flow rate and the physical properties of the liquid phase on gas hold-up and mass transfer was investigated.

Only the behavior of static mixers made of perforated metal sheet was studied afterwards, since a considerable enhancement of mass-transfer rates was found with this material, due to the turbulence-promoting effect of the orifices. Five packing elements with a distance of 5 cm between packs (SM′50) and three packs located 10 cm from each other (SM′100) were employed.

Fluid-dynamic behavior

The global gas hold-up was measured by means of the manometric method using open-tube manometers; the distance between pressure taps was 20 cm with the regular packings and 45 cm with the static mixers. Figure 10 illustrates the behavior of the different configurations studied. From this graph and in the light of visual observations, the following results can be inferred:

- The packing made from perforated plate (RP′42) leads to the highest gas hold-up values, probably due to additional bubble breakage as a result of interactions with turbulent eddies produced by the orifices.
- The gas hold-up in the column filled with regular packing is higher than in the column containing the static mixers, even in the presence of the same number of packing elements (RP′42 and SM′50).

It is well known that the presence of packings increases gas void fraction in bubble columns (Potthoff and Bohnet, 1993; Tasat et al., 1995) with respect to empty bubble columns. In the column with static mixers empty sections alternate with packed sections, but it was observed that below each static mixer arriving gas bubbles coalesce, forming a considerable gas pocket. This gas accumulation together with the enhancement of gas hold-up within the packings should yield elevated gas hold-up values, contrary to what was observed.

The measurement of local gas hold-up by the conductimetric technique (Ross and Böhm, 1998) helped to explain the observed results. The experiments were performed in a square section column with ten pairs of electrodes (1.5×1.5 cm) embedded along two opposite walls of the column filled with

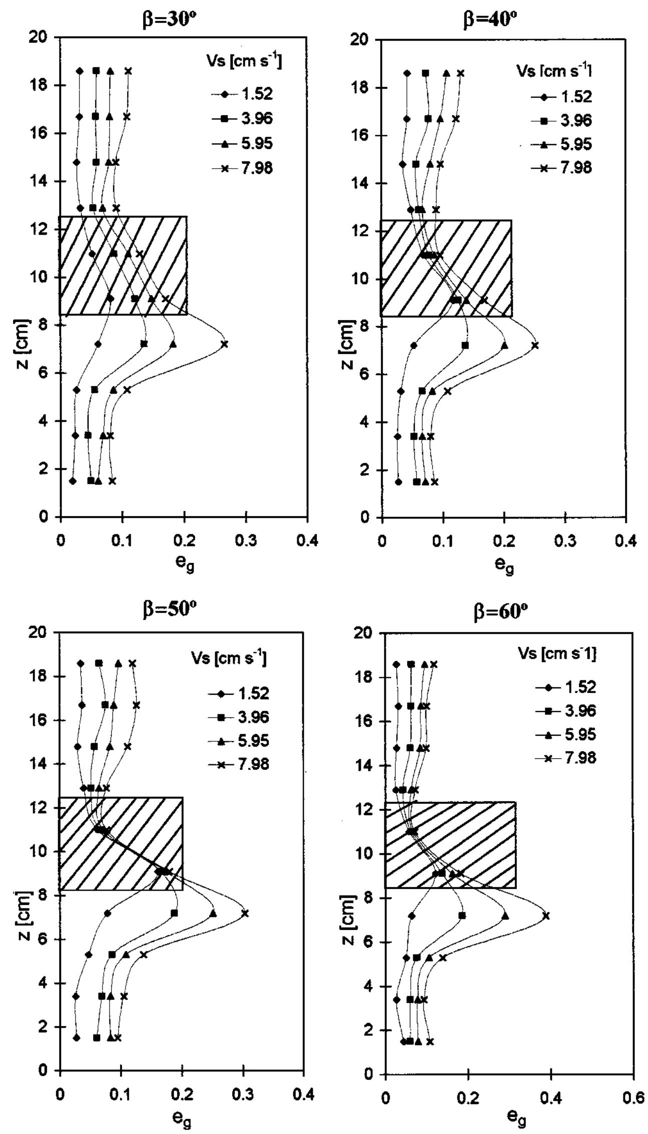

Figure 11. Local gas holdup in the axial direction for static mixers with different corrugation inclination angle.

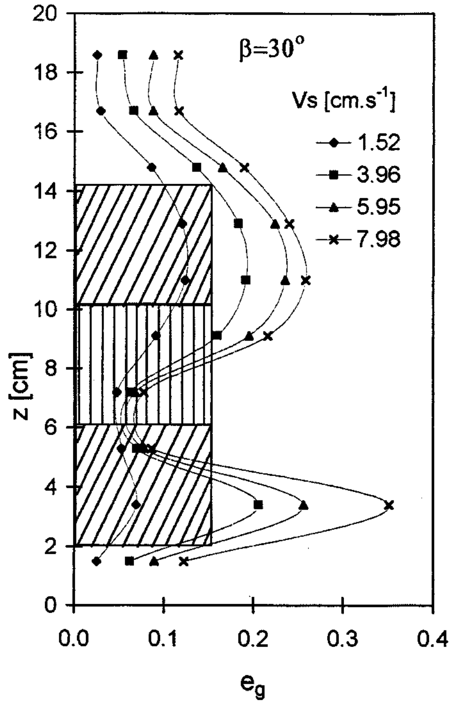

Figure 12. Local gas holdup in the axial direction within a regular packing.

plastic packing elements. The conductimeter could be connected through a selecting switch to each of the ten electrode pairs; Maxwell's equation was applied to relate the conductivity of the dispersion to the gas void fraction (Turner, 1976).

Figure 11 shows the results obtained for the static mixers placed at 8.5 cm from the gas sparger (a perforated plate with 16 orifices of 0.5 mm). It is clearly seen that gas accumulates beneath the static mixer. The local gas hold-up in this region increases with increasing gas flow rate and also with increasing corrugation inclination angle. In viscous solutions the gas accumulation is even more pronounced. It can also be seen that the gas void fraction within the packing element is drastically reduced to very small values, being almost independent of the gas superficial velocity. The single mixer element seems to work as an ejector; instead, when there are more packs stacked together (Figure 12), after the initial reduction, gas hold-up increases again, reaching values much higher than those produced in the empty column downstream of the packing. Although static mixers are often used to improve the radial gas hold-up distribution in columns and piping, the gas void fraction inside the mixing element is small and not comparable to the values obtained under similar conditions in regular packings.

Mass transfer

As shown in Figure 13, mass-transfer results obtained with the static mixers also differ from those found with regular packings. This is not surprising, since there is a correspondence between gas void fraction and mass-transfer coefficient (Cavatorta and Böhm, 1988). Only at low gas superficial velocities ($Vs < 1$ cm/s), where gas bubbles do penetrate freely into the pack and no gas accumulation occurs, similar mass-transfer rates are obtained.

With the regular packing made of perforated plate, mass-transfer coefficients are predicted by (Neme et al., 1997):

$$St = 0.105(Re\, Fr\, Sc^2)^{-0.268} \tag{12}$$

($N = 158$; $\delta = 4.7\%$), while by using all the experimental results obtained with the static mixers, the following correlation is derived:

$$St = 0.157(Re\, Fr\, Sc^2)^{-0.298} \tag{13}$$

($N = 35$; $\delta = 3\%$).

Figure 13 also includes the mass-transfer equation corresponding to the smooth-sheet packing RP45 (Tasat et al., 1995), in this case mass-transfer rates are on the average 74% lower than those obtained with the turbulence-promoting perforated plates.

Mass Transfer and Power Consumption

Energy dissipation is often used as a criterion for the evaluation of mass-transfer efficiency obtained in different contacting devices (Villermaux, 1988). It also proved very useful in practice for comparing mass-transfer coefficients at a fixed surface obtained under different operating conditions.

Figure 14 shows the experimental results of mass-transfer coefficients at 25°C plotted against the power dissipation per unit volume of fluid for solution S1, packings and static mixers made of smooth-metal sheet, and all the operating conditions described in this work except natural convection. To get a clearer picture only the data corresponding to the range 10–1,000 W/m^3 of power input are shown in Figure 14; the whole range investigated is given in Figure 15.

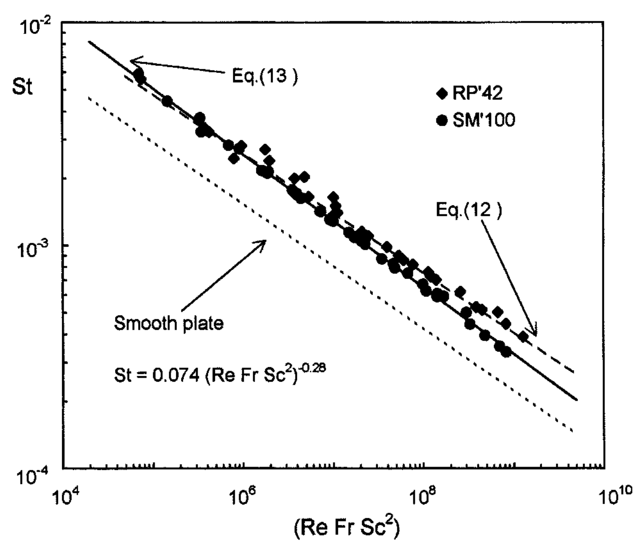

Figure 13. General correlation of mass transfer to regular packings or to static mixers in a bubble column.

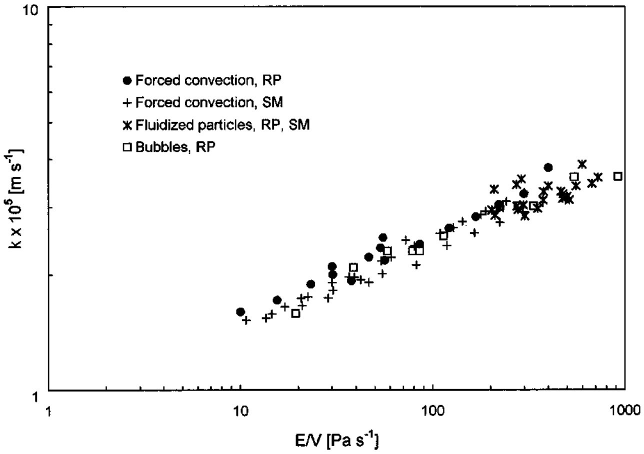

Figure 14. Mass-transfer coefficients against energetic requirements; packings and static mixers made of smooth metal sheets.

For the systems with circulating liquid the energy input per unit volume was calculated from the measured pressure drop per unit length of packing and the interstitial flow velocities, $E/V = (\Delta P/L)v$, while the energy consumption due to aeration is $E/V = \rho_L g v$.

Referring to Figure 14, it can be seen that in a fluid of given properties, a direct relationship between the density of energy dissipation and the intensity of mass transfer exists, regardless of the flow configuration involved. Power may be supplied with the purpose of producing liquid circulation or agitation by fluidized particles or by gas bubbles; increasing the power input, in every case mass-transfer efficiency is enhanced in the same way.

Figure 15 illustrates the influence of other variables on the relationship between energy input and mass-transfer coefficients. On the one hand, as expected, in order to obtain the same mass-transfer rate for a given geometry, the energy consumption increases with liquid viscosity. (In Figure 15 the viscosity of solutions S1 and S6 differs by a factor of 3.5; correspondingly, E/V varies 15 to 30 times for the same mass-transfer coefficient.) On the other hand, for the same energy supply a higher mass-transfer coefficient is found for a given configuration when perforated metal sheet is employed as a construction material. The diffusion layer developed along the transferring surface breaks down permanently at the openings, thus enhancing the mass-transfer process.

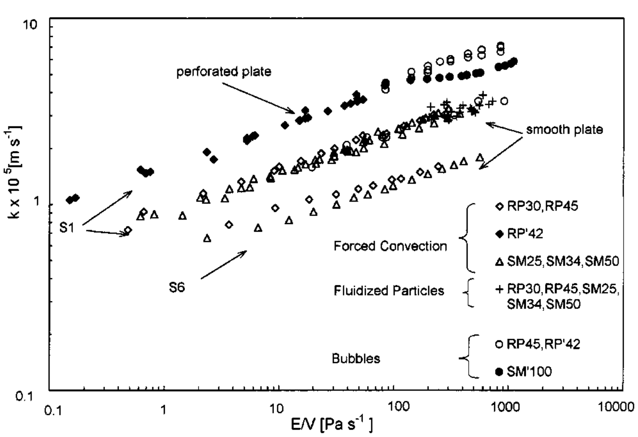

Figure 15. Mass-transfer coefficients against energetic requirements; influence of construction material and physical properties.

Another conclusion can be drawn from the results obtained with regular packing and static mixers placed in bubble columns. As can be seen, the dependence of mass-transfer coefficients on the density of energy dissipation is quite different, although the fluid properties (solution S1) and the construction material (perforated sheet) are the same. As stated elsewhere (Villermaux, 1988), in systems where the dissipated energy is only used to induce mass transfer, k should vary with $(E/V)^{0.33}$. An exponent less than 1/3 means that only a fraction of the dissipated energy is spent on mass transfer and the lower the exponent, the lower the mass-transfer efficiency of the device. In Figure 15 all the experimental points, except those corresponding to static mixers in bubble columns, fall on three nearly linear curves with a gradient of around 0.2. For the static mixers in bubble columns, k is correlated with $(E/V)^{0.1}$, indicating that much of the energy supplied is wasted without any useful effect on mass transfer. The gas accumulation beneath the packs is responsible for this behavior, since energy has to be spent again to produce new bubbles.

Concluding Remarks

An experimental investigation of fluid dynamics and mass transfer to regular packings and static mixers carried out under different convection modes showed that both internals behave similarly when they operate under free or under forced convection with and without fluidized particles. The developed mass-transfer correlations can be applied indistinctly to the packing elements stacked together or separated from each other.

In bubble columns the behavior of both configurations differs, since in the case of static mixers gas accumulation below the packing elements influences adversely the fluid dynamics and consequently the mass transfer inside the mixing device. The analysis of the relationship between energy dissipation and mass-transfer coefficient also reveals that mass-transfer efficiency of the static mixer placed in a bubble column is lower than for the other configurations and flow conditions studied.

Furthermore, alternative methods of describing mass transfer in forced flow and fluidized beds showed that the use of flow parameters defined by Bravo et al. (1986) improved the correlation of experimental data obtained in the former convection mode. Results obtained with different corrugation inclination angles could be described by a single relationship. In the presence of fluidized particles the application of those parameters is not outstanding. Results may be described by the correlations for fluid-to-wall mass transfer in fluidized beds established in the literature as well.

For all the systems (except static mixers in bubble columns), working with packing elements made from the same material and with solutions having the same properties, a direct relationship between the energy input and the mass-transfer coefficient exists, regardless of the involved flow configuration.

Acknowledgments

The financial support of the University of Buenos Aires and the National Council of Scientific and Technical Research (CONICET) is gratefully acknowledged.

Notation

a = packing surface area per unit volume, m^{-1}
d' = channel side, m
b = corrugation wavelength, m
D = diffusivity, $m^2 \cdot s^{-1}$
D' = width of corrugated plate, m
dp = particle diameter, m
E = dissipated energy, W
e = fluidized-bed voidage
e_g = volume fraction of gas
Fr = Froude number = $Vs^2 \; g^{-1} \; Z^{-1}$
g = gravitational acceleration, $m \cdot s^{-2}$
Gr = Grashof number = $g \; \Delta\rho \; Z^3 \rho\mu^{-2}$
j = j-factor for mass transfer = $Sc^{2/3} \; kv^{-1}$
j' = j-factor for mass transfer = $Sc^{2/3} \; kv'^{-1}$
k = mass-transfer coefficient, $m \cdot s^{-1}$
L = packing length, m
N = number of experimental data
ΔP = pressure drop, Pa
Re = Reynolds number = $vD_h \; \rho\mu^{-1}$
Re' = Reynolds number = $v'D'_h \; \rho\mu^{-1}$
Re_{tr} = transition Reynolds number = $vD_h \; \rho\mu^{-1}$
Re_{dp} = Reynolds number = $vdp\rho\mu^{-1}$
Sc = Schmidt number = $\mu\rho^{-1}D^{-1}$
Sh = Sherwood number = kZD^{-1}
St = Stanton number = kVs^{-1}
V = bed volume, m^3
Vs = superficial velocity, $m \cdot s^{-1}$
X = liquid-layer depth between packing elements, m
z = distance from gas distributor, m
Z = length of corrugated plate, m
α = folding angle of corrugation, deg
β = corrugation inclination angle with respect to vertical, deg
δ = mean deviation
ϵ = packing void fraction
μ = dynamic viscosity, $mPa \cdot s$
ρ = density, $kg \cdot m^{-3}$

Literature Cited

Agar, D. W., and W. Ruppel, "Multifunktionale Reaktoren für die heterogene Katalyse," *Chem. Ing. Tech.*, **60**, 731 (1988).

Böhm, U., "Maximum Mass Transfer to the Wall or Immersed Objects in Liquid Fluidized Beds," *Ind. Eng. Chem. Process Des. Dev.*, **22**, 339 (1983).

Bravo, J. L., J. A. Rocha, and J. R. Fair, "Pressure Drop in Structured Packings," *Hydrocarbon Process.*, **65**, 45 (1986).

Cavatorta, O. N., and U. Böhm, "Heat and Mass Transfer in Gas Sparging Systems: Empirical Correlations and Theoretical Models," *Chem. Eng. Res. Dev.*, **66**, 265 (1988).

Colazo, J. A., and U. Böhm, "Mass Transfer Improvements in Single Phase in Regular Packings," *Chem. Eng. Technol.*, **15**, 327 (1992).

Colazo, J. A., I. A. Nieva, and U. Böhm, "Mass Transfer to Regular Packings in Single Phase," *Chem. Eng. Technol.*, **14**, 287 (1991).

Focke, W. W., J. Zachariades, and O. Olivier, "The Effect of the Corrugation Inclination Angle on the Thermohydraulic Performance of Plate Heat Exchangers," *Int. J. Heat Mass Transfer*, **28**, 1469 (1985).

Gaiser, G., and V. Kottke, "Flow Phenomena and Local Heat and Mass Transfer in Corrugated Passages," *Chem. Eng. Technol.*, **12**, 400 (1989).

Heggs, P. J., P. Sandham, R. A. Hallam, and C. Walton, "Local Transfer Coefficients in Corrugated Plate Heat Exchanger Channels," *Chem. Eng. Res. Dev.*, **75**, 641 (1997).

Ibl, N., and R. H. Müller, "Studies of Natural Convection at Vertical Electrodes," *J. Electrochem. Soc.*, **105**, 346 (1958).

Jagannadharaju, G. J. V., and C. V. Rao, "Ionic Mass Transfer in the Presence of Fluidized Solids," *Indian J. Technol.*, **3**, 201 (1965).

King, D. H., and J. W. Smith, "Wall Mass Transfer in Liquid Fluidized Beds," *Can. J. Chem. Eng.*, **45**, 329 (1967).

Neme, F., L. Coppola, and U. Böhm, "Gas Hold-Up and Mass Transfer in Solid Suspended Bubble Columns in Presence of Structured Packings," *Chem. Eng. Technol.*, **20**, 297 (1997).

Potthoff, M., and M. Bohnet, "Einfluss statischer Mischer und des Feststoffanteils auf die Strömungsverhältinisse in Dreiphasen-Wirbelschicht-Bioreaktoren," *Chem. Ing. Tech.*, **65**, 449 (1993).

Rey, M. C., P. Glasserman, and U. Böhm, "Mass Transfer to Regular Packings at Low Reynolds Numbers and Under Natural Convection," *Ind. J. Heat Mass Transfer*, **41**, 1693 (1998).

Ross, R., and U. Böhm, "Gas-Liquid Dispersions Produced by Static Mixers," *Lat. Amer. Appl. Res.*, **28**, 175 (1998).

Selman, J. R., and C. W. Tobias, "Mass Transfer Measurements by the Limiting Current Technique," *Adv. Chem. Eng.*, **10**, 211 (1978).

Spekuljak, Z., and H. Andrada, "Some Aspects Related to Fluid Flow in Regular Geometries. Application to the Static Mixers," *Lat. Amer. Appl. Res.*, **23**, 231 (1993).

Spekuljak, Z., and R. Billet, "Pressure Gradient of the Gaseous Phase in Regular Packings," *Lat. Amer. Appl. Res.*, **19**, 133 (1989).

Spekuljak, Z., H. Monella, H. Andrada, and E. Robaina, "Structured Packing as Biological Support," *Abstracts of the Lecture Group Biotechnology*, DECHEMA (1994).

Tasat, A. I., O. N. Cavatorta, and U. Böhm, "Electrochemical Mass Transfer to Regular Packing in a Bubble Column," *J. Appl. Electrochem.*, **25**, 273 (1995).

Tonini, R. D., U. Böhm, and F. M. Brea, "Fluidization with Highly Viscous and Non-Newtonian Fluids: Mass Transfer from the Fluidized Bed to the Inner Wall of an Annulus," *Chem. Eng. J.*, **22**, 51 (1981).

Turner, J. C. R., "Two-Phase Conductivity: The Electrical Conductance of Liquid Fluidized Beds of Spheres," *Chem. Eng. Sci.*, **31**, 487 (1976).

Villermaux, J., "The Role of Energy Dissipation in Contacting and Mixing Devices," *Chem. Eng. Technol.*, **11**, 276 (1988).

Zogg, M., "Strömungs- und Stoffaustauschuntersuchungen an der Sulzer Gewebepackung," PhD Diss., Eidgenössische Technishe Hochschule (ETH), Zürich (1972).

Manuscript received June 25, 1998, and revision received Feb. 1, 1999.